Testing a new analytical approach for determination of vibrational transition moment directions in low symmetry planar molecules: 1-D- and 2-D-naphthalene

ARTICLE *in* SPECTROCHIMICA ACTA PART A MOLECULAR AND BIOMOLECULAR SPECTROSCOPY · AUGUST 2012

Impact Factor: 2.35 · DOI: 10.1016/j.saa.2012.08.046 · Source: PubMed

Spectrochimica Acta Part A: Molecular and Biomolecular Spectroscopy 98 (2012) 343–354

Contents lists available at SciVerse ScienceDirect

Spectrochimica Acta Part A: Molecular and Biomolecular Spectroscopy

journal homepage: www.elsevier.com/locate/saa

Testing a new analytical approach for determination of vibrational transition moment directions in low symmetry planar molecules: 1-D- and 2-D-naphthalene

Marin Rogojerov [a,*], Gábor Keresztury [b], Mariana Kamenova-Nacheva [a], Tom Sundius [c]

[a] Institute of Organic Chemistry, Bulgarian Academy of Sciences, 1113 Sofia, Bulgaria
[b] Chemical Research Center, Hungarian Academy of Sciences, P.O. Box 17, 1525 Budapest, Hungary
[c] Department of Physics, University of Helsinki, P.O. Box 64, FIN-00014 Helsinki, Finland

HIGHLIGHTS

- Target molecules are partially uniaxially oriented in nematic liquid crystalline solvent.
- Analytical approach gives an exact expression for calculation of orientational parameters.
- Average orientation of 1-D- and 2-D-naphthalene is slightly different from that of naphthalene.
- Transition moment directions of weak C–D bands were predicted with good accuracy.
- Mathematical method for evaluation angle between two vibrational transition moment vectors.

GRAPHICAL ABSTRACT

Testing a new analytical approach for determination of vibrational transition moment directions in low symmetry planar molecules: 1-D- and 2-D-naphthalene, partially oriented in nematic liquid crystal.

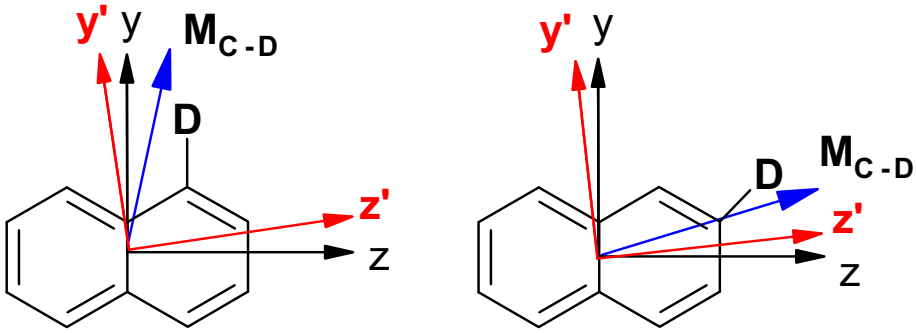

ARTICLE INFO

Article history:
Available online 24 August 2012

Keywords:
Linear dichroism
IR–LD spectra
Naphthalene
Naphthalene-d_1 isotopomers
Orientational parameters

ABSTRACT

A new analytical approach for improving the precision in determination of vibrational transition moment directions of low symmetry molecules (lacking orthogonal axes) is discussed in this paper. The target molecules are partially uniaxially oriented in nematic liquid crystalline solvent and are studied by IR absorption spectroscopy using polarized light. The fundamental problem addressed is that IR linear dichroism measurements of low symmetry molecules alone cannot provide sufficient information on molecular orientation and transition moment directions. It is shown that computational prediction of these quantities can supply relevant complementary data, helping to reveal the hidden information content and achieve a more meaningful and more precise interpretation of the measured dichroic ratios.

The combined experimental and theoretical/computational method proposed by us recently for determination of the average orientation of molecules with C_s symmetry has now been replaced by a more precise analytical approach. The new method introduced and discussed in full detail here uses a mathematically evaluated angle between two vibrational transition moment vectors as a reference. The discussion also deals with error analysis and estimation of uncertainties of the orientational parameters. The proposed procedure has been tested in an analysis of the infrared linear dichroism (IR–LD) spectra of 1-D- and 2-D-naphthalene complemented with DFT calculations using the scaled quantum mechanical force field (SQM FF) method.

* Corresponding author. Tel.: +359 02 9606 124; fax: +359 02 8700 225.
E-mail address: mrogojer@orgchm.bas.bg (M. Rogojerov).

1386-1425/$ - see front matter © 2012 Elsevier B.V. All rights reserved.
http://dx.doi.org/10.1016/j.saa.2012.08.046

Introduction

The use of polarized light in IR spectroscopy finds its main application in detection of sample orientation and symmetry assignment of the absorption bands. In these experiments, the measured infrared *linear dichroic* (IR–LD) spectra of partially oriented molecules in anisotropic solvents can also be used to determine the individual vibrational transition moment directions [1–4]. In practice, LD spectroscopy works well for determination of transition moment directions (TMDs) of molecules having C_{2v} or higher symmetry, but it encounters difficulties in this task with molecules of lower symmetry [1].

In our previous studies we have tested the feasibility and efficiency of a recently developed innovative approach for determination of the transition moments directions and the average orientation of low-symmetry planar molecules oriented in nematic liquid crystals by the combined use of IR–LD measurements and quantum-chemical calculations [5–7]. The idea to combine experimental determinations with ab initio calculations was prompted by two inherent limitations of the IR–LD experiments:

(i) The direction of the effective long axis of low-symmetry guest molecules (giving the direction of molecular alignment) is not *a priori* known and cannot be learned from IR–LD measurements alone since the vibrational transition dipole moments in low symmetry molecules have individual directions, that is, they are not oriented along molecular axes as in the case of high molecular symmetry (e.g. C_{2v}, D_{2h}) [1].
(ii) Due to the quadratic relation between the measured dichroic ratios and the orientation angles defining the TM directions (see later), the sign of these angles are not accessible from the IR–LD measurements.

Thus, in a previous communication, we solved the first problem by using extra information taken from quantum chemical prediction of the mutual orientation of two selected transition moments, i.e., an angle between two computed TM vectors lying in the molecular plane [5]. Introducing this parameter in the respective algebraic relations, the original system of two equations reduced to a complicated biquadratic algebraic equation [5]. The solution of which is the orientational parameter, K_z, defining the average orientation of the solute molecule's long axis. However, since an analytical solution was not available at that time, we have adopted a *graphical procedure* for solving it. However, in practice, the graphical solution has not proved very convenient or accurate, and has not allowed estimating the uncertainty of orientational parameter, K_z. Moreover it is not very suitable to combine observed polarization data and computationally predicted values of the angle in question for solving the mentioned above equation. Because of this, an analytical method is developed to overcome these problems.

In present article we offer an exact solution of this algebraic equation as well as an error estimation of the orientation parameter K_z. We have also developed a mathematical procedure for evaluation of the angle between the reference transition moments from the observed polarization data. The result from this approach can be used as a test to what extent the QCC can be a reliable tool for prediction of this parameter.

The performance of the new approach is then being tested with two deuterated isotopologs of naphthalene, 1-D- and 2-D-naphthalene, both having C_s symmetry. We have chosen these molecules because they have the same size and shape characteristics as the parent molecule, naphthalene, so that the orientation of all three molecules in the nematic LC phase is expected to be quite similar [8,9], while the frequencies and transition moment directions of certain vibrations will be substantially different due to the altered masses. The corresponding polarized bands in the IR–LD spectra of the two naphthalene-d_1 isotopologs are also be assigned.

Experimental details

Polycrystalline naphthalene used in this work was purchased from Aldrich (purity $\geqslant$99%), while 1-D- and 2-D-naphthalene were synthesized according to previously published procedure [10] by means of the following reaction scheme (Fig. 1).

For more details on synthesis and identification of the products see the Supplementary material. 1-D- and 2-D-naphthalene were used in this study after further purification by vacuum sublimation.

For spectral measurements of these compounds approx. 10 wt% solutions were prepared in isotropic solvent CCl_4, as well as in nematic liquid crystalline solvent ZLI-1695 (Merck). IR spectra of isotropic and anisotropic solutions were recorded on a *Nicolet Magna 750* FTIR spectrometer and a *Bruker Tensor 27* FTIR spectrometer in the 4000–400 cm^{-1} spectral region with resolution of 2 cm^{-1} using a KBr liquid cell of 25 μm path length. To achieve good uniaxial orientation of the nematic LC solution, the inner surfaces of the KBr windows were thoroughly polished to produce microgrooves running parallel to the filling direction of the liquid cell. The parallel $A_{\parallel}(\nu)$ and perpendicular $A_{\perp}(\nu)$ polarized spectra of nematic solutions and solvent were measured on both of the above mentioned instruments using Au/AgBr and Al/KRS-5 wire-grid polarizers, respectively. The dichroic ratios of individual absorption bands were determined applying the stepwise reduction procedure (described in details elsewhere [1]) using interactive spectral subtraction. Before this, the liquid crystal solvent absorption bands were almost entirely compensated from the $A_{\parallel}(\nu)$ and $A_{\perp}(\nu)$ polarized spectra of all studied substances (see Supplementary material) by means of a penalized least-squares fitting procedure developed by Eilers [11–13].

Computational methods

Quantum mechanical structure optimization of naphthalene constrained to D_{2h} symmetry and the corresponding harmonic force field and frequency calculations were done by the density functional theory (DFT) method, applying B3LYP functionals with five different basis sets: 6-31G* (#1), 6-311+G** (#2), 6-311++G** (#3), aug-cc-pVDZ (#4), and aug-cc-VTZ (#5), using the Gaussian 03 program package [14]. With two of these basis sets (6-31G* and aug-cc-VTZ) the solvent effect of the medium has also been taken into account in the DFT calculations by the use of the IEF–PCM method [15] as implemented in Gaussian 03. The optimized geometry of naphthalene for each basis set was used in the subsequent analytical evaluation of the harmonic force fields, vibrational frequencies, and dipole moment derivatives. The calculations of these molecular characteristics of 1-D- and 2-D-naphthalene have been done by simple isotopic substitution using the keyword Freq = (ReadFC, ReadIsotopes), i.e., by repeating the frequency calculation for each isotopomer with the same molecular force field but specifying the altered set of atomic masses.

The quadratic force field of naphthalene molecule obtained in Cartesian coordinates was transformed to a set of natural internal coordinates and scaled by multiple scaling factors to ensure correct assignment and a better fit of the experimental and calculated frequencies. Scaling was performed according to the SQM FF method developed by Pulay et al. [16,17], using separate scale factors for

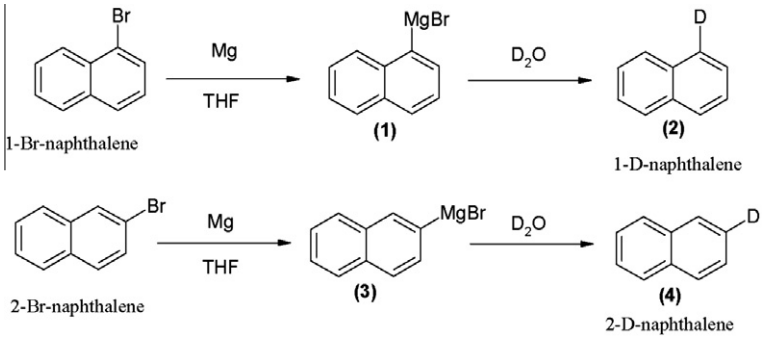

Fig. 1. Reaction scheme for synthesis of 1-D- and 2-D-naphthalene.

various types of standard internal coordinates as described by Rauhut and Pulay [18]. Least squares adjustment of the scale factors was performed in overlay calculations for the three molecules (naphthalene, 1-D- and 2-D-naphthalene), but for each chosen basis set separately. For starting values of scale factors at the B3LYP/6-31G* level, the set of values reoptimized by Baker et al. [19] has been accepted. The final sets of refined scale factors are listed in Supplementary material (see Table S1).

The transformation of the force field, its scaling and the subsequent full normal coordinate analysis including the calculation of the potential energy distributions (PED), transition moment directions, and IR and Raman intensities corresponding to the scaled force field were done with the *Molvib* program (Version 7.0) written by Sundius [20]. The simulated spectra were computed from the calculated frequency positions and intensities of naphthalene and its isotopologs using Lorentzian line shapes with 6 cm^{-1} bandwidths. They are presented in Supplementary material (Figs. S6–S11).

IR–LD spectroscopy – theoretical background

Vibrational transition moments and orientational parameters

In IR spectroscopy, light absorption is caused by molecular transitions related to the interaction between electric field of radiation and an oscillating electric dipole moment due to a change in molecular geometry during a vibration. These transitions are characterized by transition energy and absorption intensity as well as by their polarization properties determined by the transition moment directions within the molecule-fixed coordinate system.

As it is known from quantum theory of molecules, the IR intensity $A(\nu)$, or more precisely the transition probability between the ground state $|\phi_i\rangle$ and excited vibrational state $|\phi_e\rangle$ induced by light absorption, is proportional to the square modulus $|(\boldsymbol{M}, \boldsymbol{\varepsilon})|^2$ of the projection of vibrational dipole transition moment $M = \langle\phi_e|\hat{\mu}|\phi_i\rangle$ on the electric field direction $\boldsymbol{\varepsilon}$, where $\hat{\mu}$ is the dipole moment operator [21]. Therefore, transition probability is maximized when the transition moment $\boldsymbol{M}$ coincide with electric field direction $\boldsymbol{\varepsilon}$ and becomes zero when $\boldsymbol{M}$ is perpendicular to ε. This allows experimentally to determine direction of $\boldsymbol{M}$, i.e., its polarization direction, provided that the target molecule is oriented preferentially along one direction in anisotropic solvents, e.g. in nematic liquid crystals or in uniaxially stretched polyethylene [3].

In practice, this information can be extracted from the polarized IR spectra, $A_{\parallel}(\nu)$ and $A_{\perp}(\nu)$, measured at parallel and perpendicular orientation of the electric vector $\boldsymbol{E}$ of linearly polarized light to the uniaxial sample direction defined by a vector called director ($\mathbf{n}\equiv$Z) [1]. The observed intensity $A(\nu_f)$ of a certain absorption band is proportional to $\cos^2(M, \varepsilon)$, i.e., it depends on the angle (M_f, $\varepsilon\equiv$Z) between the transition moment M_f and the Z-axis of the laboratory coordinate system.[1] Since in case of (partial) uniaxial orientation the solute molecules have certain average orientation with respect to the nematic director $\mathbf{n}$, a mean orientation of the fth transition moment with respect to this direction can be described by a single parameter $K_f = \langle\cos^2(M_f, \varepsilon)\rangle$, which also depend on the alignment of the transition moments within the molecular coordinate system [1]:

$$K_f = \langle\cos^2(M_f, Z)\rangle = \sum_{u,v} K_{u,v} \cos\varphi_u^f \cos\varphi_v^f, \quad u, v = x, y, z, \tag{1}$$

where K_f is called the orientational parameter (or orientational factor) of M_f; the angle brackets $\langle,\rangle$ denote averaging over all orientations of the solute molecules, while K_{uv} are components of the orientation tensor. Factors $\cos(M_f, u) = \cos\varphi_u^f, u = x, y, z$, are direction cosines defining the orientation of the fth transition moment with respect to the molecular axes x, y, z, that make angles φ_u^f with M_f and the following relation is valid for them:

$$\cos^2\varphi_x^f + \cos^2\varphi_y^f + \cos^2\varphi_z^f = 1 \tag{2}$$

High symmetry molecules

In case of molecules of C_{2v} or higher symmetry, the evaluation of average orientation of the vibrational transition moment vectors is very straightforward since the symmetry constrains their directions along the x, y or z axes of the molecular framework (see Fig. 2a for naphthalene molecule). The corresponding orientational factors are related in a simple way to the measurable dichroic ratios that can be conveniently determined using the stepwise reduction procedure, primarily suggested by Thulstrup and Eggers[2] for processing of polarized UV–Vis spectra [22]. It is based on the following interactive subtraction operation that can be monitored visually on the computer display: $A_{\parallel}(\nu) - m \cdot A_{\perp}(\nu)$, where m is a free variable used to control the reduction process. Starting with $m \sim 0$ and gradually increasing it, all bands of one and the same polarization (of the same symmetry species) will be eliminated simultaneously when m becomes equal to the dichroic ratio, $m = R_u = A_{\parallel}/A_{\perp}$, where $u = x, y, z$, and $A_{\parallel}$ and $A_{\perp}$ are the corresponding integrated band intensities. The resulting difference spectra $A_{\parallel}(\nu) - R_u \cdot A_{\perp}(\nu)$ are known in the literature as *reduced LD spectra* [1–5].

Then, the orientational factors of the transition moments associated with the observed bands can simply be determined by the following formula [1]:

$$K_u = K_{uu} = \langle\cos^2(M_u, \varepsilon)\rangle = R_u/(2 + R_u), \quad u = x, y, z, \tag{3}$$

where R_u are the measured dichroic ratios. Since the possible TMDs coincide with one of the molecular axes x, y, z, the orientational

[1] This axis is usually used to define the uniaxial direction in nematic liquid crystals and stretched polymers.

[2] In this procedure the effect of solvent birefringence on the spectral properties of the solute is neglected.

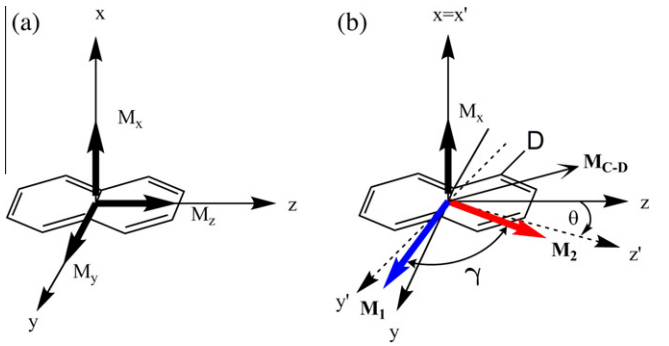

Fig. 2. Distribution of vibrational transition moment directions: (a) in highly symmetric (D_{2h}) naphthalene molecule and (b) in low symmetry planar (C_s) molecule 1-D-naphthalene. $\mathbf{M_1}$ and $\mathbf{M_2}$ are reference transition moments, while γ is the angle between them. The angle θ defines a rotation of arbitrarily chosen axes to principal axes system.

tensor $\boldsymbol{K}$ acquires a diagonal form: $K_{uv} = K_{uu}\,\delta_{uv}$, whereas the trace of $\boldsymbol{K}$ is equal to one:

$$Tr(\boldsymbol{K}) = K_x + K_y + K_z = 1. \tag{4}$$

For the sake of simplicity, the following notation is adopted: $K_u = K_{uu}$, ($u = x, y, z$).

If the molecule has a brick-like shape, as in the case of naphthalene, the following relation is valid for orientational parameters: $K_x \leqslant K_y < K_z$. This means that the average direction of the z-axis[3] of the molecular frame has the largest possible value of K, while the other two directions (y and x) have lower order of orientation with respect to the unique sample axis Z.

Based on the determined K_u values, the band polarization can in most cases be unambiguously determinated by stepwise reduction procedure allowing to assign observed absorption bands to the corresponding IR-active symmetry species (see IR–LD spectra of naphthalene in the Section "Results and discussion").

Low symmetry molecules

When a molecule has no symmetry, the vibrational transition moments are not fixed by symmetry, so they may have individual directions and, at the same time, the location of the long axis z of the molecule-fixed coordinate system (x, y, z) also becomes indefinite [1]. This fact hampers the determination of the average orientation of solute molecules and of their transition moment directions. Therefore, additional information is required to locate the average direction of the "long" molecular axis. Several attempts or approximate methods to circumvent this problem are described in the literature [23–26]; however, none of them solved this task successfully. In order to solve this non-trivial problem correctly, we need to determine all non-zero components of orientational tensor K_{uv}.

In our studies we consider the simplest case of low symmetry molecules, i.e., planar molecules having C_s point group symmetry. In this case tensor $\boldsymbol{K}$ should have three independent unknown elements, K_x, K_{yz} and K_z, while $K_y = 1 - (K_x + K_z)$ (see Eq. (4)). The direction out-of-plane transitions (coincides with the x-axis) is defined uniquely (see 1-D-naphthalene, Fig. 2b). Their corresponding orientational parameter K_x can be determined experimentally in a straightforward way by stepwise reduction of the measured polarized IR spectra as $K_x = R_x/(2 + R_x)$ [1]. However, the situation is more complex for determination of the orientation of in-plane transition moments since their individual directions are lying somewhere in the molecular plane and their orientational factors can be defined as follows (see also Eq. (3)):

$$K_f = K_{yy}\sin^2\varphi_f + K_{zz}\cos^2\varphi_f + 2K_{yz}\sin\varphi_f\cos\varphi_f, \tag{5}$$

where $\cos\varphi_f$ and $\sin\varphi_f$ are direction cosines describing the transition moment orientation in the plane (see Eq. (2)), while K_{yy}, K_{zz} and K_{yz} are orientational parameters of solute in arbitrary molecular framework (or in our case, in a coordinate system used in quantum chemical calculations). The number of unknown components of K_{uv} can be reduced using a principal molecular axis system (x', y', z'). It can be achieved by rotation of arbitrary molecular coordinate system around the fixed axis $x{\equiv}x'$ perpendicular to the molecular plane, by a certain angle, θ (see Fig. 2b). As a consequence of this rotation, $K_x = K_{x'}$ and the orientational parameters $K_{y'}$ and $K_{z'}$ remain unknown only, since in principal axis framework all off-diagonal elements become zero and the orientational matrix has a diagonal form, $K_{uv} = K_{uu}\,\delta_{uv}$ [1]. Then, the orientation parameter K_f of any in-plane transition moment, M_f, can be represented by the expression:

$$K_f = K_{y'}\sin^2\varphi'_f + K_{z'}\cos^2\varphi'_f, \tag{6}$$

where $\varphi'_f = \varphi_f + \theta$. Thus angles φ'_f and φ_f define the transition moment orientations in the principal axes system and in an arbitrary one (e.g. in the coordinate system used in quantum chemical calculations), respectively.

If the direction of the long molecular axis z' and its orientation parameter $K_{z'}$ are somewhere known , then due to Eq. (4) $K_{y'}$ is also known[4], and the transition moment direction of each in-plane vibration, defined by angle φ'_f (see Eq. (6)) can be determined from the experimental dichroic data by the use of relation $K_f = R_f/(2 + R_f)$ (see Eq. (3)) and the following equation [1]:

$$\tan(\varphi'_f) = \pm\sqrt{\frac{K_{z'} - K_f}{K_f - K_{y'}}}, \quad \text{where } K_{z'} \geqslant K_f \geqslant K_{y'}, \tag{7}$$

This formula implies two important limitations:

(i) *The sign ambiguity of* φ'_f: the signs of φ'_f are not accessible from experiment (see Eq. (7)), only the absolute value $|\varphi'_f|$ can be obtained, so one cannot tell whether the transition moment makes an angle φ'_f with the z' axis clockwise or counter-clockwise.

(ii) *Imperfection of* $K_{z'}$ *experimental estimation*: although we know that $K_{z'} \geqslant \max(K_f)$, (where *max* ($K_f$) is the largest K_f value obtained from the measured dichroic ratios), it is very probable that none of the in-plane transition moments will coincide with the z' direction. Nonetheless, max (K_f) can be used as a reliable lower limit value of $K_{z'}$.

Graphical approach to determine $K_{z'}$

As it was shown in our previous study, the task for determination of the $K_{z'}$ and $K_{y'}$ values cannot be unambiguously solved without the prior knowledge of at least the *mutual orientation* of two selected transition moments, M_1 and M_2 (in the molecular plane), defined by angle γ (see Fig. 2b) [5]. The corresponding vibrational modes should have fairly strong absorption bands and notably different K_f values ($f = 1, 2$). Then, to find the orientational parameters $K_{y'}$ and $K_{z'}$ in the new reference axes y' and z', a set of two equations (like Eq. (6)) written for the orientational factors K_1 and K_2 must be solved. This leads to the following algebraic equation [5]:

[3] It is called the effective orientational axis or is frequently named "long" molecular axis.

[4] For example when the transition moment corresponding to the band with the highest measured dichroic ratio occasionally coincides with the effective long axis.

$$\tan(\gamma) = f(K_{z'}) = \frac{\sqrt{\frac{K_{z'}-K_2}{K_2-(a-K_{z'})}} - \sqrt{\frac{K_{z'}-K_1}{K_1-(a-K_{z'})}}}{1+\sqrt{\frac{K_{z'}-K_2}{K_2-(a-K_{z'})}}\sqrt{\frac{K_{z'}-K_1}{K_1-(a-K_{z'})}}}, \quad (8)$$

which can be solved for $K_{z'}$, assuming that γ is known parameter.

The following substitutions $a = 1 - K_{x'}$ and $a - K_{z'} = K_{y'}$ have been used, where $K_{x'}$, K_1 and K_2 are experimental data determined by the measured dichroic ratios R_x, R_1 and R_2 according to Eq. (3).

Since experimental information on angle γ is rarely available [26], a theoretical source, i.e., *ab initio* or DFT quantum chemical predictions were used to estimate an approximate value. The sought parameter $K_{z'}$ have been found by solving graphically Eq. (8) in our previous studies [5–7].

Analytical solution for $K_{z'}$

The graphical solution was found to be a somewhat inconvenient way of solving Eq. (8), so efforts were made to solve it analytically. There are also two further reasons:

The first one stems from the fact that the uncertainties in determination of K_1 and K_2 are not always small enough, particularly at partial overlap of close-lying bands, or inaccurate solvent absorption compensation. In these cases the graphical approach does not provide dependable results for K_z. The uncertainties of K_1 and K_2 cannot be easily evaluated by means of Eq. (8).

The second reason is connected with the combined use of experimental and computationally predicted polarization data in Eq. (8). This raises the question whether quantum chemical calculations can be used as a reliable tool for prediction of vibrational transition moment directions (and the angles between them). One of the aims of our work is to clarify this question.

As we can see below, the exact solution of Eq. (8) may improve the reliability of this determination and help overcome these problems to a certain extent.

Introducing the substitution $p = \tan(\gamma)$ and after a series of mathematical transformations of Eq. (8), the following biquadratic equation is obtained:

$$\left(K_{z'}-\frac{a}{2}\right)^4 - \left(K_{z'}-\frac{a}{2}\right)^2\left(\frac{(1+p^2)^2}{4.p^2}(K_1+K_2-a)^2 - \frac{(1+p^2)}{p^2}\left(K_1-\frac{a}{2}\right)\left(K_2-\frac{a}{2}\right)\right) = 0, \quad (9)$$

This equation has four roots:

$$\text{One is twofold}: K_{z'_{1,2}} = \frac{a}{2} \quad (10)$$

while the other two can be obtained by some simplifications in the form:

$$K_{z'_{3,4}} = \frac{a}{2} \pm \frac{1}{2}\sqrt{(1+p^2)(K_1+K_2-a)^2 + \frac{(1+p^2)}{p^2}(K_1-K_2)^2} \quad (11)$$

However, only one of these roots fulfills the condition $K_f \leqslant \underline{K_z} \leqslant a - K_x$, ($f = 1, 2$), namely:

$$K_{z'} = \frac{a}{2} + \frac{1}{2} \times \sqrt{(1+\tan^2\gamma)(K_1+K_2-a)^2 + \frac{(1+\tan^2\gamma)}{\tan^2\gamma}(K_1-K_2)^2} \quad (12)$$

Estimation of absolute transition moment directions

Once a more realistic value of $K_{z'}$ is obtained from Eq. (12), one can evaluate the experimental angles φ'_f between each transition moment M_f and the principal z'-axis using Eq. (7), where angles φ'_f can assume any value in the interval $-90^\circ \geqslant \varphi'_f \leqslant +90^\circ$. However, due to the sign ambiguity of φ'_f: only their absolute values $|\varphi'_f|$ can be obtained from experiment: $0^\circ \leq |\varphi'_f| \leq 90^\circ$. To resolve this problem we may take extra information comparing the angles $|\varphi'_f|$ with those predicted by quantum chemical calculations φ_f^{calc}. This can be achieved by choosing one and the same frame via coordinate transformation of either the system of principal axes (x', y', z') used in the experiment or the coordinate system (x, y, z) used in the quantum chemical calculations.[5] However, the most correct way to do this is to rotate the coordinate system (x, y, z) in the (y, z) plane by an appropriate angle θ, since the signs of the experimentally determined angles φ'_f are not known and cannot be subjected to this transformation, as it could lead to large errors. Thus, all calculated TM vectors would be rotated consistently, in the same direction, so that $\varphi_f^{calc} = \varphi_{f,o}^{calc} + \theta$, where θ is calculated by the differences of corresponding reference TM angles: $|\varphi_r^{calc} - \varphi'_1| \sim |\varphi_2^{calc} - \varphi'_2| \approx \theta$ while $\varphi_{f,o}^{calc}$ are initially predicted angles taken in the frame of the quantum chemical calculations [5]. One should then compare the corresponding values of $|\varphi_f^{calc}|$ with the experimental data $|\varphi'_f|$ based on proper assignment of the calculated to the measured frequencies (aided also by the relative intensities). At this point many of these angles should come close to each other, $|\varphi_f^{calc}| \sim |\varphi'_f|$, at least for the strong bands. Then the signs of the corresponding observed angles can be determined by $\varphi_f^{obs} = |\varphi'_f|.sgn(\varphi_f^{calc})$ and a correlation graph of φ_f^{obs} vs. φ_f^{calc} can be prepared (see in Section "Predicted transition moment directions").

Uncertainty estimation of K_z parameter

As it can be seen from Eq. (12), K_z is a function of several variable parameters, but three of them, *tan* (γ), K_1 and K_2, play an important role in its uncertainty estimation. The value of K_x is already determined and its uncertainty usually exceeds the statistical error of measurement that can affect the third decimal [9]. It is obvious that the uncertainty of K_z is a generic function of the uncertainties of the above mentioned quantities. However, the contribution of uncertainty of angle γ cannot be directly estimated since there are no experimental data which can be compared with theoretically predicted ones. As it will be shown below in Section "Results and discussion", the K_z parameter varies very slowly with angle γ, so that the predicted accuracy of K_z parameter depends mainly on uncertainties of K_1 and K_2 parameters. Thus, γ will have a fixed value while K_z will depend only on two parameters, K_1 and K_2, and has a minimum $K_{z-min} = (1 - K_{x'})/2$ at $K_1 = K_2 = (1 - K_{x'})/2$; Therefore, the following expression can be written for estimation of the uncertainty of K_z [28]

$$\sigma_{K_z} = \sqrt{\sigma_{K_1}^2\left[\frac{\partial K_z}{\partial K_1}\right]^2 + \sigma_{K_2}^2\left[\frac{\partial K_z}{\partial K_2}\right]^2}, \quad (13)$$

where σ_{K_1} and σ_{K_2} are uncertainties of K_1 and K_2, respectively, while $\frac{\partial K_z}{\partial K_1}$ are $\frac{\partial K_z}{\partial K_2}$ are derivatives of K_z with respect to these parameters (they are given in the Supplementary material).

In the absence of spectral overlap or artifacts from solvent spectrum miscompensation they may also due to the local field effect [27], the uncertainties in determination of K_f ($f = 1, 2$) are usually of the order $\sigma_{K_f} \leqslant 0.005$ [8]. Then, on the basis of this assumption we can estimate the error, σ_{K_z} from Eq. (13). We should note that the uncertainties of K_1 and K_2 can be individually determined by similar approach applied to formula 3. The uncertainties of dichroic ratios σ_{R_1} and σ_{R_2} can be evaluated by standard statistical analysis [28].

[5] For example the "standard orientation" in Gaussian.

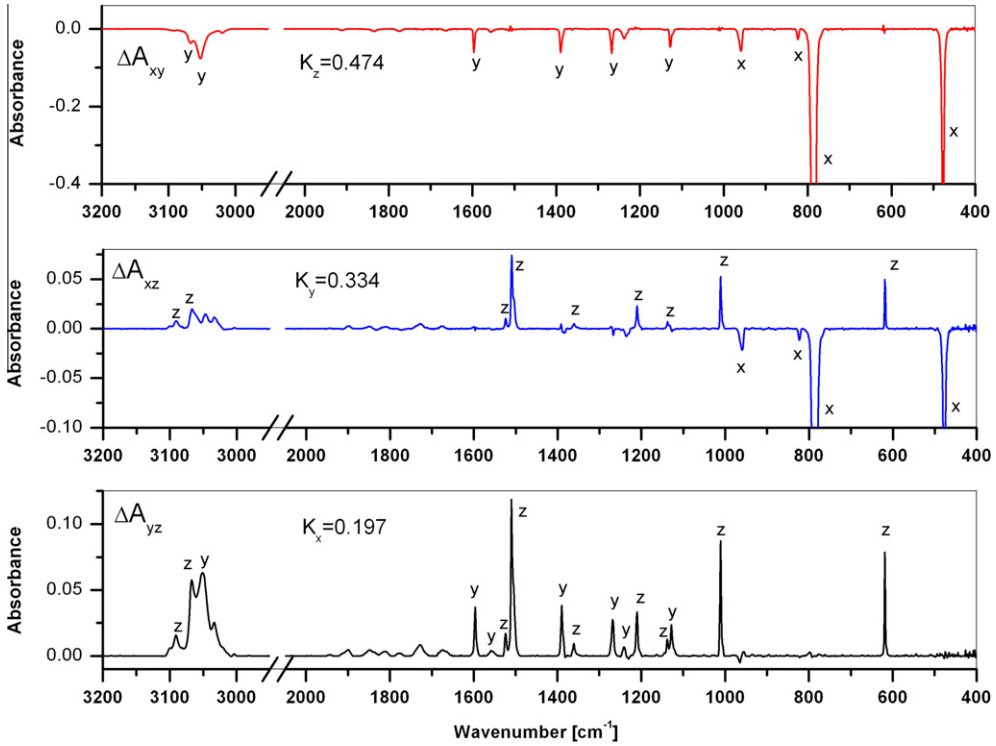

Fig. 3. Reduced IR–LD spectra, ΔA_{xy}, ΔA_{xz}, and ΔA_{yz}, of a 10% (m/m) nematic solution of naphthalene; subscripts indicate polarization directions of bands that remain observable after elimination of other bands during interactive subtraction. The K_i ($i = x, y, z$) values are the orientational parameters obtained from the dichroic ratios determined by application of the stepwise reduction procedure.

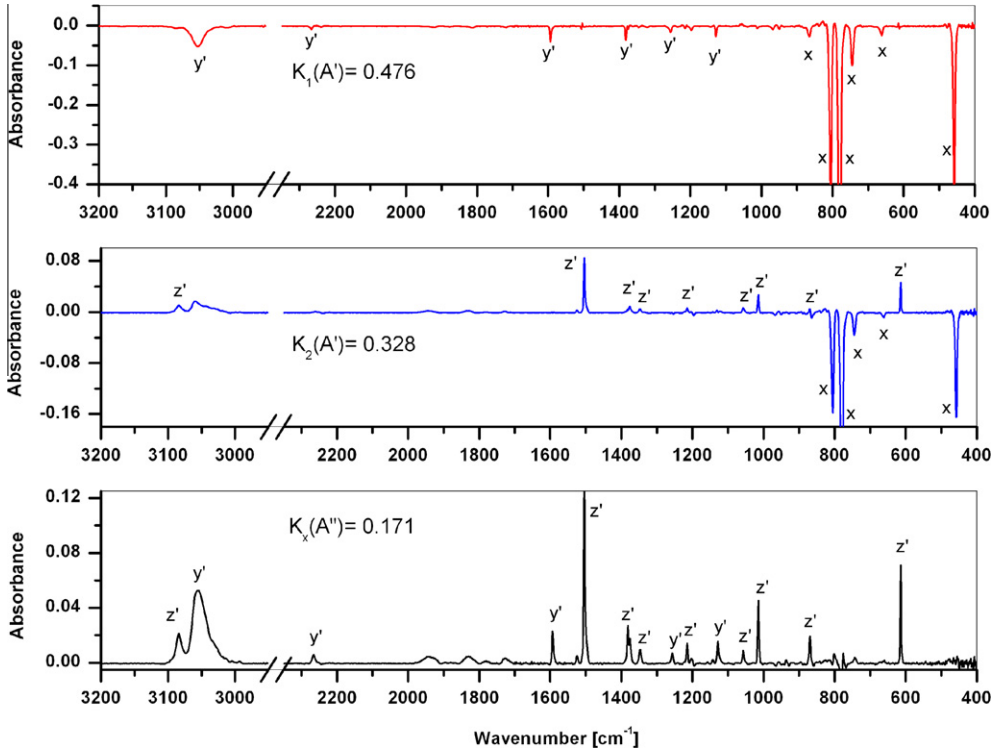

Fig. 4. Reduced IR–LD spectra of 1-D-naphthalene in 10% nematic solution in ZLI-1695. Superscript '-prime (in y' and z') denotes similar band polarization behavior as in the parent molecule of D_{2h} symmetry, i.e., "y-like" and "z-like" polarization. The subtraction factors 0.476 and 0.328 were chosen to be similar to K_z and K_y values of naphthalene and they are related to its in-plane transitions of B_{1u} and B_{2u} species, respectively, while $K_x = 0.171$ corresponds to out-of-plane (B_{3u}) transitions. The determinated orientational parameters of 1-D-naphthalene are $K_z = 0.494$ and $K_y = 0.334$.

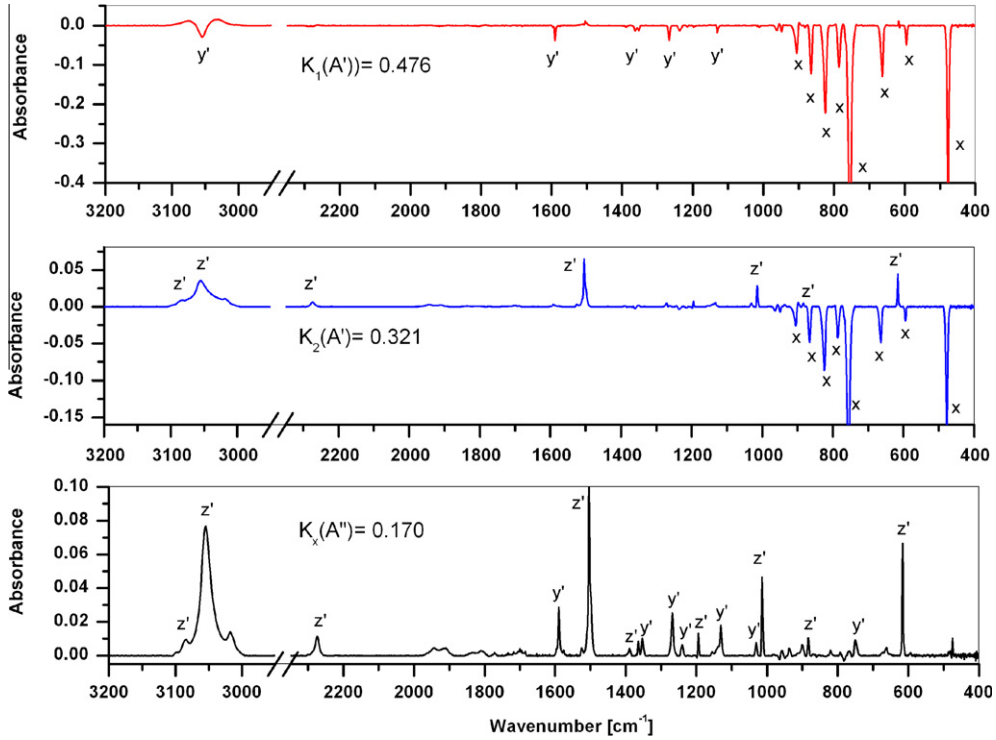

Fig. 5. Reduced IR–LD spectra of 2-D-naphthalene in 10% nematic solution in ZLI-1695. Subscript '-prime (in y' and z') denotes similar band polarization behavior as in the parent molecule of D_{2h} symmetry, i.e., "y-like" and "z-like" polarization. The subtraction factors 0.476 and 0.321 were chosen to be similar to K_z and K_y values of naphthalene and they are related to its in-plane transitions of B_{1u} and B_{2u} species, respectively, while $K_x = 0.172$ corresponds to out-of-plane (B_{3u}) transitions. The determinated orientational parameters of 2-D-naphthalene are $K_z = 0.495$ and $K_y = 0.333$.

Results and discussion

Since the spectral [29–31] and orientational [32–34] characteristics of naphthalene are very well studied, this molecule is used in the present work as a good illustration for investigation of the change of these features when the molecular symmetry is lowered from D_{2h} to C_s by selective H–D isotopic substitutions (see Fig. 1).

Frequency assignment

Isotropic and polarized IR spectra of naphthalene, 1-D- and 2-D-naphthalene were recorded and compared for assigning the observed absorption bands to different vibrational modes. The reduced IR–LD spectra measured in nematic LC solution are given in Figs. 3–5. They were used to determine the dichroic ratios, orientational parameters and symmetry assignments of the allowed vibrational transitions. The respective experimental and computational spectral data are listed and compared in Tables 1–3 along with the assignments of bands to different normal modes. The isotropic IR spectra of naphthalene isotopologs observed in CCl_4 solution and KBr pellet as well as the simulated spectra of these molecules based on SQM FF predictions (of fundamental frequencies and intensities) together with the experimental Raman and polarized IR spectra are additionally presented in Supplementary material (see full band assignment in Tables S2–S4).

The equilibrium geometry of the free molecule of naphthalene is planar and belongs to D_{2h} point group symmetry; it has 48 normal modes of vibrations that are distributed among the symmetry species available under D_{2h} symmetry as follows [29–31]:

$$\Gamma(D_{2h}) = 9A_g + 3B_{1g} + 4B_{2g} + 8B_{3g} + 4A_u + 8B_{1u} + 8B_{2u} + 4B_{3u},$$

where the 24 g-modes are all Raman-active, 20 u-modes are infrared active, and the remaining 4 A_u modes are completely inactive. The IR-active vibrations belong to symmetry species B_{1u}, B_{2u} and B_{3u}, whereas the absorption bands (see Fig. 6) due to in-plane vibrations are polarized either along the y-axis (B_{1u}) or the z-axis (B_{2u})[6], while those due to out-of-plane vibrations are polarized perpendicular to the plane, along the x-axis (B_{3u}), as illustrated in Fig. 2a. Our detailed band assignment is presented in Table 1.

Several authors have dealt with the assignment of naphthalene vibrational spectra in the past [29–31]. The most recent spectral data of this molecule are published by Cané et al. [31], so we have compared our experimental results from isotropic and polarized measurements with the latter frequency assignments.

On isotopic exchange of one of the H atoms with a D atom in position 1 or 2 in naphthalene molecule (see Fig. 1) its symmetry changes from D_{2h} to C_s and the fundamental vibrations of 1-D-naphthalene and 2-D-naphthalene are distributed among the new symmetry species as:

$$\Gamma(C_s) = 33A' + 15A'',$$

where all normal modes are infrared and Raman active (see Tables 2 and 3 and Tables S3–S4). The previously Raman-active but IR-forbidden A_g and B_{3g} modes now become allowed in IR as in-plane polarized A' transitions, while the former B_{1g}, B_{2g}, and inactive A_u modes of naphthalene are transformed to out-of-plane polarized A'' transitions in the selectively monodeuterated isotopomers (see also the correlation diagram in Fig. 6).

The symmetry lowering of naphthalene on selective deuteration is revealed not only by the appearance of new infrared and Raman active bands but also by the observable change in polarization directions of in-plane vibrational bands best characterizing the isotopic exchange in 1-D- and 2-D-naphthalene: the C–D stretching

[6] There is a difference in our notation of symmetry species and those recommended by IUPAC (Pure & Appl.Chem. 69 (1997) 1641–1649). This is due to the difference in molecular coordinate system definition. In our molecular frame z is chosen to coincide with the long axis. In many cases such a chosen coordinate system does not correspond with IUPAC recommendations.

Table 1
In-plane IR active normal modes of naphthalene calculated by the SQM FF method at B3LYP/6-311++G** level, and orientation parameters K_f of observed band polarization directions derived from IR to LD measurements.

Mode No.	Experimental					Calculated				
	Sym. species	ν (cm^{-1}) IR and Ra[a]	ν (cm^{-1}) IR–LD	ν (cm^{-1}) CCl_4	K_f	ν (cm^{-1})	$\varphi_{c,f}$ (deg.)	$M_{y,f}$	$M_{z,f}$	PED (%)
17	$8B_{1u}(y)$	3062	3053 m	3054	0.345	3054	90	−7.4574	−0.0003	νCH(99)
18		3040	3038 sh	–	–	3037	90	−2.2397	0.0003	νCH(99)
19		1602	1597 m	1598	0.335	1602	90	1.7144	0.0000	νCC(67), βCH(27), αCCC(6)
20		1389	1390 m	1391	0.343	1389	90	2.1044	0.0000	βCH(78), νCC(17), αCCC(5)
21		1272	1268 m	1269	0.329	1261	90	−2.6141	0.0000	βCH(49), νCC(31), αCCC(20)
22		1127	1128 m	1128	0.334	1128	90	2.4125	0.0001	βCH(43), νCC(29), αCCC(27)
23		796	–	–	–	793	90	0.4021	0.0000	αCCC(71), νCC(24), βCH(5)
24		359	–	–	–	358	90	−1.2417	0.0000	αCCC(74), νCC(21)
29	$8B_{2u}(z)$	3067	3067 sh	3068	–	3065	0	−0.0003	6.3389	νCH(99)
30		3048	3046 sh	3047	–	3041	0	0.0000	−0.9381	νCH(99)
31		1514	1510 m	1509	0.475	1514	0	0.0000	−2.8359	νCC(55), βCH(41)
32		1362	1361 w	1361	0.429	1361	0	0.0000	−0.8579	νCC(70), βCH(28)
33		1212	1210 w	1210	0.474	1207	0	0.0000	−0.8800	νCC(63), βCH(37)
34		1142	1138 vw	1138	0.472	1147	0	−0.0002	0.9584	βCH(57), νCC(42)
35		1009	1011 m	1012	0.471	1011	0	0.0000	−3.0486	νCC(82), βCH(16)
36		617	619 m	618	0.473	624	0	0.0000	1.8304	αCCC(91)

Comments: $\varphi_{c,f}$ are calculated angles between transition moments and long (z) molecular axis; $M_{y,f}$ and $M_{z,f}$ are y and z components of fth transition moment M_f in the coordinate system used in DFT calculations; PED is potential energy distribution.
[a] Combined values from IR spectrum of 10% CCl_4 solution and/or from Raman spectrum of polycrystalline powder.

Table 2
In-plane normal modes of 1-D-naphthalene calculated by scaled quantum mechanical SQM FF method at B3LYP/6-311++G** force field level and orientation parameter K_f of observed band polarization directions from IR to LD measurements.

Mode No.	Experimental				Calculated				
	ν (cm^{-1}) IR and Ra[a]	ν (cm^{-1}) IR–LD	K_f	$\lvert\varphi_{p,f}\rvert$ (deg.)	ν (cm^{-1})	$\varphi_{c,f}$ (deg.)	$M_{y,f}$	$M_{z,f}$	PED (%)
1	3068	3069 w	0.394	52.5	3067	−6.7	0.4051	−3.4770	νCH(99)
2	3062	3061	0.365	64.3	3066	15.7	−1.4689	−5.2240	νCH(99)
3	3056	3054 m	–	–	3055	−88.2	5.5701	−0.1779	νCH(99)
4	3047	–	–	–	3052	−78.8	3.5461	−0.7000	νCH(99)
5	3041	3039	–	–	3043	0.2	−0.0019	−0.6367	νCH(99)
6	3030	–	–	–	3040	−70.6	1.3751	−0.4831	νCH(99)
7	3022	–	0.340	79.8	3038	84.3	−1.3061	−0.1297	νCH(99)
8	**2269**	2266 w	–	–	2252	−80.0	−2.5263	0.4442	νCD(96)
9	1625	–	0.334	–	1630	−55.7	0.2660	−0.1814	νCC(66), αCCC(17), βCH(16)
10	1591	1593 m	0.403	49.2	1599	83.1	1.5797	0.1913	νCC(68), βCH(24), αCCC(7)
11	1570	1573 vw	0.483	15.2	1573	37.1	0.0903	0.1194	νCC(72), αCCC(14), βCH(14)
12	1502	1504 m	–	–	1509	−1.3	0.0630	−2.6867	νCC(55), βCH(40)
13	1458	1460 w	–	–	1458	−37.8	−0.0780	0.1005	βCH(57), νCC(37), αCCC(5)
14	1436	–	0.333	–	1443	−69.2	−0.1928	0.0732	βCH(57), νCC(36)
15	1381	1382 m	0.377	59.1	1382	−85.1	2.1563	−0.1843	βCH(64), νCC(29), αCCC(5)
16	1376	1375 sh	0.390	54.0	1366	−50.2	0.3119	−0.2598	νCC(90), βCH(6)
17	1347	1346 w	0.303	–	1348	60.1	−1.1130	−0.6404	νCC(72), βCH(21)
18	1260	1256 w	0.422	42.3	1255	87.4	−1.9693	−0.0880	βCH(52), νCC(27), αCCC(20)
19	1214	1215 w	0.279	–	1217	41.5	0.6711	0.7570	νCC(49), βCH(34), αCCC(14)
20	1200	1199 vw	0.492	6.4	1199	−43.7	−0.3922	0.4105	βCH(53), νCC(40), αCCC(6)
21	1159	1157 vw	0.419	43.4	1160	−10.2	0.0600	−0.3341	βCH(79), νCC(18)
22	1145	1142 vw	0.339	80.9	1147	−16.4	0.1817	−0.6156	βCH(60), νCC(38)
23	1127	1128 wm	0.369	62.5	1129	81.7	2.0917	0.3057	βCH(43), νCC(31), αCCC(25)
24	1055	1057 w	0.486	12.9	1059	54.6	−0.9439	−0.6702	νCC(61), βCH(25), βCD(10)
25	1011	1014 m	0.466	24.8	1015	2.5	−0.1085	−2.4877	νCC(81), βCH(17)
26	937	937 vw	0.430	39.3	935	−24.2	0.3444	−0.7661	αCCC(82), νCC(13)
27	**869**	869 wm	–	–	868	−33.4	0.9263	−1.4028	**βCD(61)**, νCC(25), αCCC(11)
28	784	794	0.191	–	794	78.5	−0.3409	−0.0691	αCCC(70), νCC(24)
29	746	745 m	0.493	4.5	737	−52.0	−0.1955	0.1529	νCC(68), αCCC(21), βCD(7)
30	614	614 m	–	–	622	−0.2	0.0077	−1.8185	αCCC(91)
31	510	–	–	–	509	−29.0	0.0186	−0.0336	αCCC(87), νCC(10)
32	507	508 vwb	–	–	507	−67.7	0.0658	−0.0270	αCCC(58), νCC(39)
33	355	–	–	–	353	2.5	1.1997	0.0358	αCCC(73), νCC(21)

Comments: $\lvert\varphi_{p,f}\rvert$ and $\varphi_{c,f}$ are predicted and calculated angles between transition moments and long (z) molecular axis; $M_{y,f}$ and $M_{z,f}$ are y and z components of fth transition moment M_f in coordinate system used in DFT calculations; PED is potential energy distribution.
[a] Combined values from IR spectrum of 10% CCl_4 solution and/or from Raman spectrum of polycrystalline powder.

(ν_{C-D} at 2266 and 2274 cm^{-1}), C–C–D in-plane bending bands (β_{C-D} at 869 and 883 cm^{-1}, respectively) in the anisotropic LC solutions. Their mixing with the other stretching and bending vibrations is reflected by the PED data in Tables 2 and 3, providing a valuable insight in the altered conditions of vibrational couplings. Note that the C–D out-of-plane bending vibrations (γ_{C-D} at 661 and 662 cm^{-1} in the 1-D- and 2-D-derivatives, respectively) preserve their out-of-plane polarization direction (characterized by low orientation factors, around 0.170) under the lowered C_s point group symmetry as well.

Table 3
In-plane normal modes of 2-D-naphthalene calculated by Scaled Quantum Mechanical SQM FF method at B3LYP/6-311++G** force field level and orientation parameter K_f of observed band polarization directions from IR to LD measurements.

Mode No.	Experimental				Calculated				
	ν (cm^{-1}) IR and Ra[a]	ν (cm^{-1}) IR–LD	K_f	$\lvert\varphi_{p,f}\rvert$ (deg.)	ν (cm^{-1})	$\varphi_{c,f}$ (deg.)	$M_{y,f}$	$M_{z,f}$	PED (%)
1	3069	3069 sh	0.453	30.6	3066	−2.1	0.1534	−4.2415	νCH(99)
2	3061	3062 sh	0.391	53.3	3059	45.9	−3.5274	−3.4168	νCH(99)
3	3057	3055 s	0.361	65.4	3054	−87.1	5.3721	−0.2751	νCH(99)
4	3048	–	–	–	3045	−74.0	2.7720	−0.7928	νCH(99)
5	3043	3043 sh	0.361	65.4	3041	−87.7	1.9745	−0.0761	νCH(99)
6	3035	–	0.454	30.2	3039	−59.6	−1.7366	1.0180	νCH(99)
7	3029	3017 w	0.402	49.3	3036	74.2	−0.8991	−0.2552	νCH(99)
8	**2271**	2274 w	0.431	38.9	2259	−36.7	−1.5894	2.1358	**νCD(96)**
9	1625	1628 vw	0.338	79.9	1630	−89.4	0.3279	−0.0032	νCC(66), αCCC(17), βCH(17)
10	1587	1590 m	0.337	81,0	1595	−87.9	1.4576	−0.0528	νCC(68), βCH(24), αCCC(6)
11	1576	1573 vw	0.438	36.4	1575	−16.3	0.0585	−0.2005	νCC(72), αCCC(14), βCH(13)
12	1502	1504 s	0.488	12.0	1508	−3.8	0.1783	−2.7059	νCC(56), βCH(39)
13	1456	1449	–	–	1454	−6.8	0.0093	−0.0784	βCH(68), νCC(30)
14	1437	1437 w	–	–	1438	−72.2	−0.8775	0.2809	βCH(49), νCC(41), αCCC(6)
15	1381	1390 vw	0.355	68.4	1368	82.5	0.2832	0.0373	νCC(93)
16	1363	1364 w	0.353	69.5	1363	58.9	−1.1186	−0.6750	νCC(54), βCH(42)
17	1355	1353 w	0.351	70.5	1355	−62.3	−1.0655	0.5587	νCC(52), βCH(36), βCD(7)
18	1269	1268 m	0.337	81.0	1261	−89.8	−2.6152	0.00762	βCH(48), νCC(31), αCCC(21)
19	1238	1239 w	0.371	61.0	1241	−47.2	0.1042	−0.0966	βCH(58), αCCC(21), νCC(20)
20	1196	1195 w	0.494	4.5	1195	−7.6	0.1211	−0.9116	νCC(63), βCH(35)
21	1157	1155 vw	0.429	39.7	1155	−37.7	0.2935	−0.3798	βCH(72), νCC(26)
22	1141	1142 vw	0.493	6.4	1146	−2.6	0.0351	−0.7693	βCH(61), νCC(38)
23	1130	1131 w–m	0.336	82.2	1132	83.9	−2.0837	−0.2219	βCH(48), νCC(30), αCCC(22)
24	1027	1031 w	0.457	29.0	1028	−33.3	0.6235	−0.9487	νCC(66), βCH(24), βCD(7)
25	1011	1014 m	0.49	10.1	1015	−6.7	0.3155	−2.6872	νCC(80), βCH(16)
26	950	938 vw	0.394	52.2	935	49.2	0.3376	0.2917	αCCC(86), νCC (7)
27	**881**	883 w–m	0.392	52.9	881	45.3	−0.9264	−0.9153	**βCD(59)**, νCC(24), αCCC(16)
28	784	–	–	–	779	−74.2	0.1962	−0.0557	αCCC(63), νCC(27), βCD(6)
29	746	–	–	–	747	48.8	0.0725	0.0634	νCC(64), αCCC(23), βCD(9)
30	614	616 m	0.494	4.5	622	0.7	−0.0213	−1.8663	αCCC(90)
31	511	–	–	–	509	−4.7	−0.0022	0.0266	αCCC(75), νCC(22)
32	505	–	–	–	504	−17.9	0.0036	−0.0111	αCCC(76), νCC(21)
33	355	–	–	–	355	88.9	−1.2472	−0.0231	αCCC(73), νCC(22)

Comments: $\lvert\varphi_{p,f}\rvert$ and $\varphi_{c,f}$ are predicted and calculated angles between transition moments and long (z) molecular axis; $M_{y,f}$ and $M_{z,f}$ are y and z components of fth transition moment M_f in coordinate system used in DFT calculations; PED is potential energy distribution.
[a] Combined values from IR spectrum of 10% CCl_4 solution and/or from Raman spectrum of polycrystalline powder.

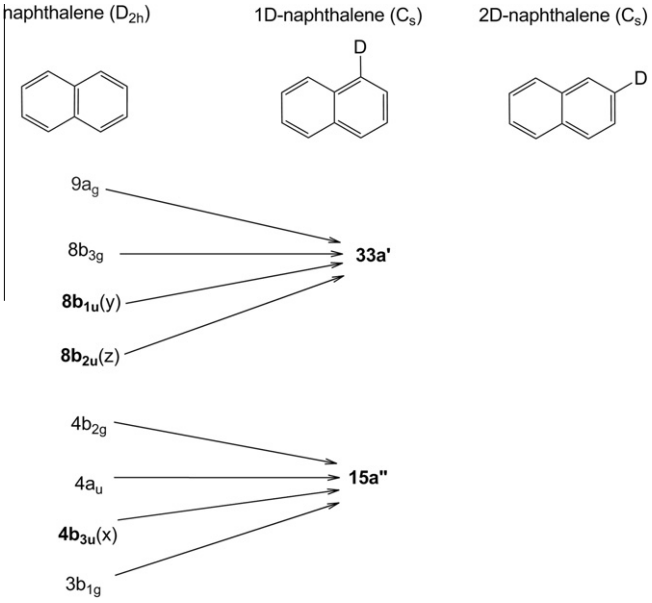

Fig. 6. Correlation diagram between the symmetry species of naphthalene, D_{2h}, and 1-D- and 2-D-naphthalene, C_s. The symmetry species of IR active transitions are denoted by bold letters.

Principally, for molecules having C_s symmetry, the out-of-plane (A'') vibrations can be distinguished most easily from the in-plane (A') modes by the use of reduced IR–LD spectra [1–5]. However to assess the similarity between IR–LD spectra of naphthalene (Fig. 3) with those of 1-D- and 2-D-naphthalene, we prepared three reduced IR–LD spectra with subtraction factors chosen to be close to the dichroic ratios measured for non-substituted naphthalene (see Figs. 4 and 5).

The good agreement between the calculated and experimentally observed frequencies allows us to assign adequately some low intensity bands of 1-D-naphthalene (at 784 and 737 cm^{-1}) and of 2-D-naphthalene (at 779 and 747 cm^{-1}), too (see Figs. 4 and 5 and also Tables 2 and 3).

The results of IEF–PCM frequency calculations have shown that the solvent effects have no remarkable influence and do not really improve the frequency fit (see Tables 4 and 5) at such low dielectric constants of the medium ($\varepsilon_d \approx 5$ for the nematic solvent). At these conditions, optimization of the scaling factors may account for both the anharmonic correction and solvent effects in a certain extent. It allows the scaled quantum mechanical force field calculations to be used in this case conveniently for frequency prediction instead of the time consuming IPCM or IEF–PCM solvation model calculations at the same level of theory.

Orientational parameters

In order to calculate the K_z parameter of solute molecules by the use of Eq. (12) (see Section "Analytical solution for $K_{z'}$") it is necessary to know not only the values of orientational parameters K_1 and K_2 of two selected transition moments M_1 and M_2 lying in the molecular plane but also their mutual orientation given by

Table 4
Reference transition moment directions φ_i(deg.), (i = 1, 2) and their difference $\gamma = \varphi_2 - \varphi_1$ of both isotopomers of naphthalene are predicted by DFT calculations at different levels of theory. The frequencies ν_i (cm^{-1}) of these transitions are given in separate columns. Experimental φ and γ values are evaluated from measured dichroic ratio data.

Method/level	1-D-naphthalene					2-D-naphthalene				
	ν_2	φ_2	ν_1	φ_1	γ	ν_2	φ_2	ν_1	φ_1	γ
B3LYP/6-31G*	1127	80.3	623	−0.1	80.4	1131	84.5	626	0.4	84.1
B3LYP/6-311+G**	1127	81.7	620	−0.2	81.9	1132	83.9	622	0.6	83.3
B3LYP/6-311++G**	1129	81.7	622	−0.2	81.9	1132	83.9	622	0.7	83.2
B3LYP/aug-cc-pVDZ	1133	81.6	622	−0.2	81.8	1137	85.2	624	0.5	84.7
B3LYP/aug-cc-pVTZ	1127	81.2	618	−0.3	81.5	1131	82.7	620	0.5	82.2
B3LYP/6-31G*/IEF PCM	1127	78.8	623	−0.2	79.0	1128	84.5	623	0.2	84.2
B3LYP/aug-cc-pVTZ/IEF PCM	1127	79.0	623	−0.3	79.3	1128	83.3	623	0.3	83.0
Experimental	1127	80.9	614	−4.5	85.4	1131	82.4	616	−4.0	86.4

Comments: the sign of experimentally determined values of φ_1 and φ_2 are taken from QCC.

Table 5
Transition moment directions, φ (deg.), of the C–D stretching and C–D in-plane bending vibrations of the two monodeuterated naphthalene isotopomers predicted by DFT calculations at different levels of theory. The frequencies ν (cm^{-1}) of these transitions are given in separate columns. The experimental φ values are evaluated from measured dichroic ratio data.

Method/level	1-D-naphthalene				2-D-naphthalene			
	ν_s(C–D)	φ_s	ν_b(C–D)	φ_b	ν_s(C–D)	φ_s	ν_b(C–D)	φ_b
B3LYP/6-31G*	2251	−78.3	866	−38.4	2259	−34.3	880	52.1
B3LYP/6-311+G**	2251	−80.1	866	−33.4	2259	−36.6	881	44.5
B3LYP/6-311++G**	2251	−80.0	866	−33.4	2259	−36.7	881	45.3
B3LYP/aug-cc-pVDZ	2251	−80.9	867	−33.0	2260	−36.7	880	43.5
B3LYP/aug-cc-pVTZ	2251	−80.8	866	−33.7	2259	−36.5	880	44.5
B3LYP/6-31G*/IEF PCM	2250	−77.4	866	−35.2	2260	−40.6	877	51.9
B3LYP/aug-cc-pVTZ/IEF PCM	2251	−80.2	865	−38.4	2259	−50.2	878	43.8
Experimental	2269	−79.8	869	−39.3	2271	−38.9	881	52.9

Comments: the sign of experimentally determined values of φ_s and φ_b (for C–D stretching and bending modes) are taken from QCC.

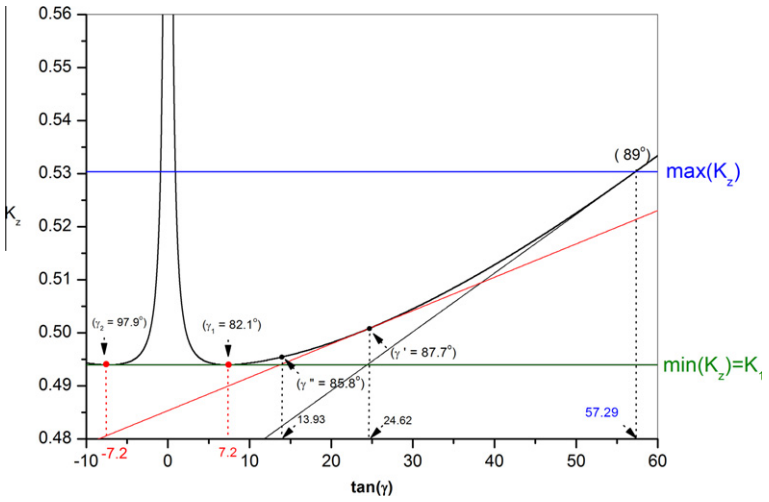

Fig. 7. The dependence of K_z on tan(γ). The minimum of K_z function, min (K_z) = K_1 is assigned by green color solid line at $\tan(\gamma_1) = \pm\sqrt{\frac{K_1-K_2}{K_1+K_2-a}}$, where $a = 1 - K_x$. The maximum value of K_z, max(K_z) is defined by blue solid line which crosses the K_z function at point (γ = 89°). The approximated value of $\gamma = \gamma''$ (85.8° for 1-D-naphthalene and 86.4° for 2-D-naphthalene) is obtained by application of Newton–Raphson method.

the angle γ. Since experimental data for this angle are not available, its approximated values for the two isotopomers can be evaluated by searching for the minimum of the function: $\frac{dK_z}{d\tan(\gamma)} = 0$ (the derivative of Eq. (12) is given in the Supplementary material).

Function $K_z = f(\tan(\gamma))$ has two very shallow minima, $\min(K_z) = K_1$ at $\tan(\gamma_i) = \pm\sqrt{\frac{K_1-K_2}{K_1+K_2-a}}$ (see Fig. 7), γ_i, i = 1,2; $a = 1 - K_x$, where the sought angle γ can be found in their vicinity. The values of angles γ_i for both isotopomers were found to be similar (82.1, 97.9 for 1-D-naphthalene and 83.6, 96.4 for 2-D-naphthalene) since the corresponding values of K_1 and K_2 for the selected reference transitions at 623 and 1127 cm^{-1} turn out to be very similar. These transitions were chosen since on isotopic substitution the corresponding TMDs change their z and y components only slightly in the molecule-fixed coordinate system (see Tables 4 and 5) and also because of their negligible overlap with other bands. In principle, transitions whose directions do not undergo a considerable change after isotopic exchange can be used as candidates for a reference pair and their orientational parameters must satisfy additionally the following conditions: $K_1 > K_2$ and $K_1 + K_2 > a = 1 - K_x$.

Since the sought angle γ can be found in one of two intervals: $\gamma_1 > \gamma > 90°$ or $\gamma_2 < \gamma < 90°$ (see Fig. 7), the predicted values of angle γ^{calc} from our DFT calculations give a hint that tan (γ^{calc}) > 0 (see

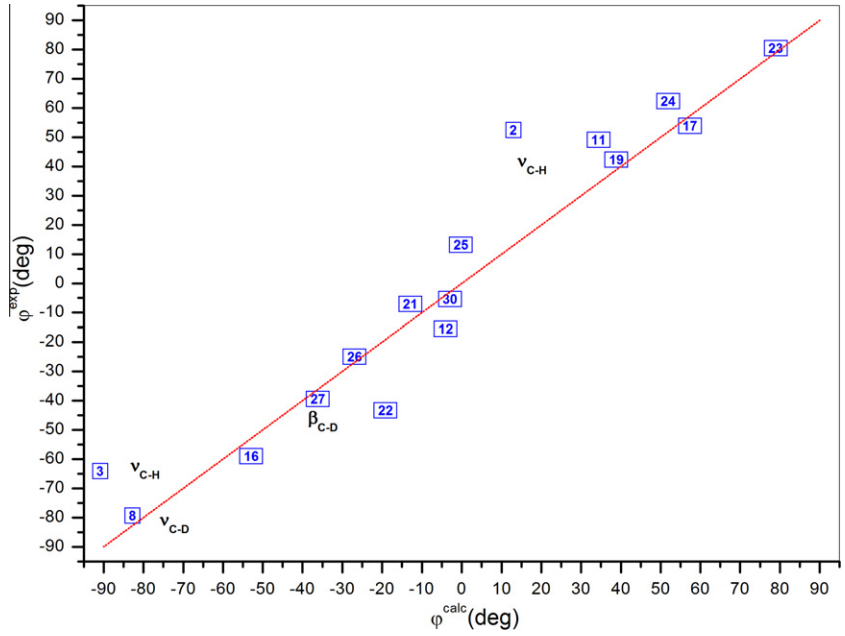

Fig. 8. 1-D-naphthalene: correlation between calculated φ_f^{calc} and experimentally determined transition moment directions $\varphi_f^{exp} \equiv \varphi_f'$ in the principal axis system. The φ_f^{calc} values were obtained by means of $\varphi_f^{calc} = \varphi_{f,o}^{calc} + \theta$, where $\theta \sim -3°$ while $\varphi_{f,o}^{calc}$ are initially predicted angles taken in the frame of the QCC.

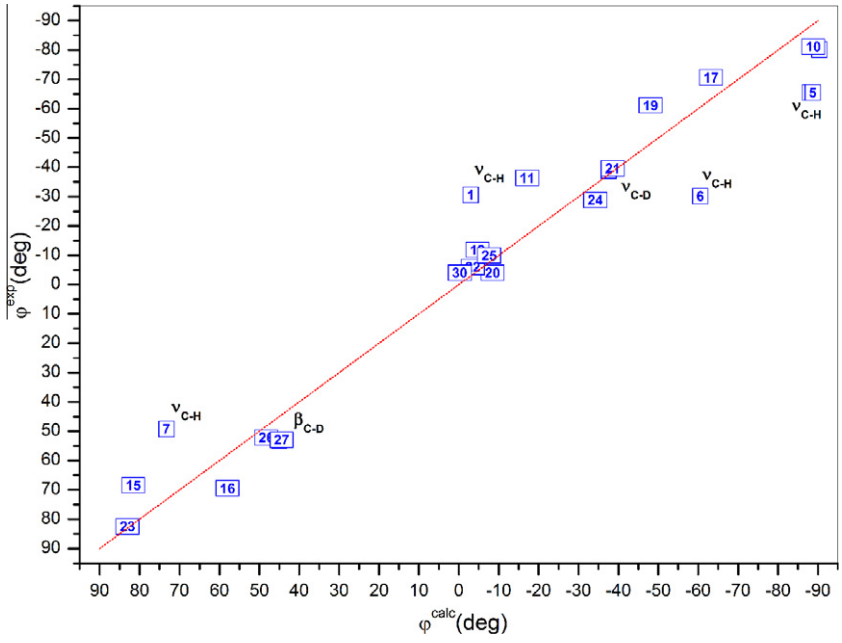

Fig. 9. 2-D-naphthalene: correlation between calculated φ_f^{calc} and experimentally determined transition moment directions $\varphi_f^{exp} \equiv \varphi_f'$ in the principal axis system. The φ_f^{calc} values were obtained by means of $\varphi_f^{calc} = \varphi_{f,o}^{calc} + \theta$, where $\theta \sim -1°$ while $\varphi_{f,o}^{calc}$ are initially predicted angles taken in the frame of the QCC.

Table 4), i.e., γ can be located in the interval $\gamma_1 = 82.1 < \gamma \leqslant 89°$, but its value should be nearby to γ_1 (see Fig. 7), since $K_z \geqslant \max(K_f) = K_1$. Then, an approximate value of γ can be found in this interval by the use the Newton–Raphson method for root estimation of function $K_z = f(\tan(\gamma))$. Only two steps[7] are required to estimate the sought value of γ, where as a starting point in this iterative procedure, $(\tan(89°), \max(K_z))$ were used (see Fig. 7).

There is a certain distinction of few (3–5) degrees between the theoretically predicted values of γ and those obtained by the use of the proposed method (see Table 4). However, we should note that this difference is not so big and is in the frame of expected uncertainty of γ which depends on the uncertainties of both parameters K_1 and K_2.

The determined values for K_z parameters of 1-D-naphthalene ($K_z = K_z$=0.494 ± 0.008, $K_y = K_y$ = 0.335 ± 0.008, K_x = 0.171 ± 0.005) and 2-D-naphthalene (K_z = 0.495 ± 0.007, K_y = 0.333 ± 0.007, K_x = 0.172 ± 0.005) are somewhat different from those of naphthalene (K_z = 0.474 ± 0.005, K_y = 0.343 ± 0.005, K_x = 0.180 ± 0.005). This difference in their average orientation is obviously due to isotopic exchange, i.e., to mass effect, since the three molecules have identical molecular shape characteristics that suggest the same behavior at

[7] The next step leads to a very close value for parameter Kz∼K1, so their difference is in the fourth decimal, i.e., much smaller than the uncertainty of the determination.

their alignment in liquid crystalline solvent [35,36]. The uncertainties of determination of the K_z and K_y values are always the same and calculated from Eq. (13).

Predicted transition moment directions

Utilizing the already calculated K_z parameter value, the transition moment directions of all in-plane (A') vibrations were determined by means of Eq. (13). The result of the comparison between the experimentally obtained angles ϕ'_f and the theoretically predicted angles are shown in Figs. 8 and 9. The large deviations from the dotted line (corresponding to ideal coincidence) may be explained by inaccuracy of dichroic ratio determination due to overlapped bands and/or artifacts from imperfect compensation (subtraction) of the solvent spectrum. On the other hand they may be due to the ability of the QCC method to predict the directions of some transition moments accurately, but not all of them (see Figs. 8 and 9).

Conclusions

(1) In contrast to our previously developed graphical approach, the present analytical method gives an exact expression for calculation of orientational parameter K_z, by means of which the uncertainty of determination of K_z can be evaluated as a function of uncertainties of parameters K_1 and K_2.
(2) A mathematical approach for evaluation of the angle between reference transition moments carefully selected from the measured polarization data is also developed.
(3) The values obtained for the K_z parameter of 1-D-naphthalene and 2-D-naphthalene are slightly different from that of naphthalene. The differences are clearly due to the mass effect of isotopic substitution.
(4) Computational predictions of vibrational spectra according to the SQM FF method (multiple scaling of the force field) using the B3LYP hybrid density functional in conjunction with five different basis sets, all proved similarly successful in providing feasible vibrational frequencies for all fundamentals of naphthalene and its two D_1-isotopologs. With a refined set of 6 force-constant scaling factors, the r.m.s. frequency errors were between 6.9 and 8.1 cm^{-1} (well below 1%) in all cases.
(5) An improved method showed interesting results especially for the pair of in-plane C–D stretching and C–D bending bands in the IR spectra of the two D_1-isotopologs of naphthalene as well as for the respective TMDs. While the overall correlation between the experimentally observed and computationally predicted TMDs was not as good as in case of polar molecules having strong absorption bands (see e.g. Refs. [6,7]), it is remarkable that the TMDs of the characteristic but rather weak ν(CD) and β(CD) bands were predicted with surprisingly good accuracy (within ± (1–5)°, even at the lowest level of theory applied (B3LYP/6-31G*, SQM force field).
(6) The use of solvation (SCRF) models in the calculations (e.g. the IEF–PCM method, to account for the influence of the dielectric effect of the liquid crystalline solvent used in the IR–LD measurements) introduced 0–15° changes in various calculated TMDs, but these changes did not improve the correlation. The currently available SCRF models are able to account to a certain extent for the anisotropic solvent effects on the transition moment directions of the solute molecule. Perhaps an anisotropic version of the IEF–PCM method would be more suitable for this purpose.

Acknowledgements

M.R. and G.K. thank the Bulgarian and Hungarian Academies of Sciences for supporting a bilateral project in the field of vibrational spectroscopy of partially oriented molecules in nematic solvents using polarized light. We also thank Dr. Eidenschink (Nematel, Mainz, Germany) for donating us a small amount of nematic liquid crystal ZLI-1695.

Appendix A. Supplementary data

Supplementary data associated with this article can be found, in the online version, at http://dx.doi.org/10.1016/j.saa.2012.08.046.

References

[1] J. Michl, E.W. Thulstrup, Spectroscopy with Polarized Light, VCH, New York, 1986.
[2] B. Jordanov, M. Rogojerov, B. Schrader, J. Mol. Struct. 408 (409) (1997) 309.
[3] T. Thormann, M. Rogojerov, B. Jordanov, E.W. Thulstrup, J. Mol. Struct. 509 (1999) 93.
[4] M. Rogojerov, B. Jordanov, G. Keresztury, J. Mol. Struct. 480/481 (1999) 153.
[5] M. Rogojerov, G. Keresztury, B. Jordanov, J. Mol. Struct. 661–662 (2003) 227.
[6] M. Rogojerov, G. Keresztury, B. Jordanov, Spectrochimica Acta Part A 61 (2005) 1661.
[7] G. Keresztury, M. Rogojerov, Bulg. Chem. Commun. 37 (2005) 327.
[8] J.G. Radziszewski, V. Balaji, P. Carsky, E.W. Thulstrup, J. Phys. Chem. 95 (1991) 5064.
[9] J.G. Radziszewski, J.W. Downing, M.S. Gudipati, V. Balaji, E.W. Thulstrup, J. Michl, J. Am. Chem. Soc. 118 (1996) 10275.
[10] H. Gilman, N. John, F. Schulze, Organic Syntheses Coll. 2 (1943) 425; H. Gilman, N. John, F. Schulze, Organic Syntheses Coll. 11 (1931) 80.
[11] P.H.C. Eilers, Anal. Chem. 75 (2003) 3299.
[12] P.H.C. Eilers, Anal. Chem. 76 (2004) 404.
[13] H.F.M. Boelens, R.J. Dijkstra, P.H.C. Eilers, F. Fitzpatrick, J.A. Westerhuis, J. Chromatogr. A 1057 (2004) 21.
[14] M.J. Frisch, G.W. Trucks, H.B. Schlegel, G.E. Scuseria, M.A. Robb, J.R. Cheeseman, J.A. Montgomery Jr., T. Vreven, K.N. Kudin, J.C. Burant, J.M. Millam, S.S. Iyengar, J. Tomasi, V. Barone, B. Mennucci, M. Cossi, G. Scalmani, N. Rega, G.A. Petersson, H. Nakatsuji, M. Hada, M. Ehara, K. Toyota, R. Fukuda, J. Hasegawa, M. Ishida, T. Nakajima, Y. Honda, O. Kitao, H. Nakai, M. Klene, X. Li, J.E. Knox, H.P. Hratchian, J.B. Cross, C. Adamo, J. Jaramillo, R. Gomperts, R.E. Stratmann, O. Yazyev, A.J. Austin, R. Cammi, C. Pomelli, J.W. Ochterski, P.Y. Ayala, K. Morokuma, G.A. Voth, P. Salvador, J.J. Dannenberg, V.G. Zakrzewski, S. Dapprich, A.D. Daniels, M.C. Strain, O. Farkas, D.K. Malick, A.D. Rabuck, K. Raghavachari, J.B. Foresman, J.V. Ortiz, Q. Cui, A.G. Baboul, S. Clifford, J. Cioslowski, B.B. Stefanov, G. Liu, A. Liashenko, P. Piskorz, I. Komaromi, R.L. Martin, D.J. Fox, T. Keith, M.A. Al-Laham, C.Y. Peng, A. Nanayakkara, M. Challacombe, P.M.W. Gill, B. Johnson, W. Chen, M.W. Wong, C. Gonzalez, J.A. Pople, Gaussian 03, Revision B.05, Gaussian, Inc., Pittsburgh, PA, 2003.
[15] J. Tomasi, B. Mennucci, R. Cammi, Chem. Rev. 105 (2005) 2999–3093.
[16] P. Pulay, G. Fogarasi, G. Pongor, J.E. Boggs, A. Vargha, J. Am. Chem. Soc. 105 (1983) 7037.
[17] G. Fogarasi, X. Zhou, P.W. Taylor, P. Pulay, J. Am. Chem. Soc. 114 (1992) 8191.
[18] G. Rauhut, P. Pulay, J. Phys. Chem. 99 (1995) 3093; G. Rauhut, P. Pulay, Correction: ibid. 99 (1995) 14572.
[19] J. Baker, A.A. Jarzecki, P. Pulay, J. Phys. Chem. A 102 (1998) 1412.
[20] T. Sundius, J. Mol. Struct. 218 (1990) 321; T. Sundius, Vib. Spectrosc. 29 (2002) 89.
[21] P.W. Atkins, Molecular Quantum Mechanics, second ed., Oxford University Press, 1993.
[22] E.W. Thulstrup, J.H. Eggers, Chem. Phys. Lett. 85 (1968) 690.
[23] B. Norden, Chem. Scr. 1 (1971) 145.
[24] Y. Tanizaki, S.I. Kubodera, J. Mol. Spectrosc. 24 (1967) 1.
[25] K.R. Popov, Opt. Spectrosc. 39 (1975) 142.
[26] J. Waluk, E.W. Thulstrup, Chem. Phys. Lett. 135 (1987) 515; J. Spanget-Larsen, J. Waluk, E.W. Thulstrup, J. Phys. Chem. 94 (1990) 1800.
[27] E.M. Aver'yanov, Zh. Eksp. Teor. Fiz. 103 (1993) 2018; E.M. Aver'yanov, JETP 76 (1993) 1002.
[28] M. Caria, Measurement Analysis: An Introduction to the Statistical Analysis of Laboratory Data in Physics, Chemistry and the Life Sciences, Imperial College Press, London, 2000.
[29] S.S. Mitra, H.J. Bernstein, Can. J. Chem. 37 (1959) 553.
[30] H. Sellers, P. Pulay, J.E. Boggs, J Am. Chem. Soc. 107 (1985) 6487.
[31] E. Cané, A. Miani, A. Trombetti, J. Phys. Chem. A 111 (2007) 8218.
[32] A. Davidsson, B. Norden, Chem. Phys. Lett. 28 (1974) 221.
[33] M. Lamotte, J. Chim. Phys. PCB 72 (1975) 803.
[34] E.W. Thulstrup, J. Michl, J. Am. Chem. Soc. 104 (1982) 5594.
[35] D.S. Zimmerman, E.E. Burnell, Mol. Phys. 78 (1993) 678.
[36] A. Ferrarini, G.J. Moro, P.L. Nordio, G.R. Luckhurst, Mol. Phys. 77 (1992) 1.